applied sciences

MDPI

*Article*

# Design and Analysis of Photon Imaging Detector Based on Printed Circuit Board Technology Cross Strip Anode

**Jinyao Duan [1,2], Jinkun Zheng [1,*], Yang Yang [1,*], Yuchao Song [3], Anpeng La [3] and Yonglin Bai [1,2]**

[1] Key Laboratory of Ultrafast Photoelectric Diagnostic Technology, Xi'an Institute of Optics and Precision Mechanics (XIOPM), Chinese Academy of Sciences, Xi'an 710119, China; duanjinyao21@mails.ucas.ac.cn (J.D.); baiyonglin@opt.ac.cn (Y.B.)
[2] University of Chinese Academy of Sciences (CAS), Beijing 100049, China
[3] School of Electronic Engineering, Xi'an University of Posts and Telecommunications, Xi'an 710119, China; 2643737051@stu.xupt.edu.cn (Y.S.); ampadd@stu.xupt.edu.cn (A.L.)
* Correspondence: zhjink@opt.ac.cn (J.Z.); yangyang@opt.cn (Y.Y.)

**Abstract:** Detectors with cross strip (XS) anodes have high application value in deep space exploration, quantum communications, space astronomical telescopes, etc. In this article, a single-layer XS anode based on Printed Circuit Board (PCB) technology is proposed, which can conveniently realize large-area array detection with a simple process and low cost. We theoretically studied the electron motion principle and equivalent model of the XS anode and established a model of the XS anode through the finite element method. The model allows us to determine the anode geometry, such as anode strip width, inter-strip distance, and substrate thickness, to optimize the output signal on the XS anode, thereby indirectly affecting the resolution of the detector. The optimal parameters of the detector were processed with the help of our model, such as a strip width of 110 μm, strip spacing of 550 μm, and substrate thickness of 150 μm. The model shows that the strip charge collection ratio is 1:1. Comparing model predictions with experimental measurements reveals key parameters, such as the manufacturing is convenient and simple and can provide some ideas for subsequent large-area array detector imaging.

**Keywords:** UV; position-sensitive anode; finite element method

check for updates

**Citation:** Duan, J.; Zheng, J.; Yang, Y.; Song, Y.; La, A.; Bai, Y. Design and Analysis of Photon Imaging Detector Based on Printed Circuit Board Technology Cross Strip Anode. *Appl. Sci.* **2023**, *13*, 12304. https://doi.org/10.3390/app132212304

Academic Editor: Chi-Wai Chow

Received: 23 October 2023
Revised: 7 November 2023
Accepted: 8 November 2023
Published: 14 November 2023

**Copyright:** © 2023 by the authors. Licensee MDPI, Basel, Switzerland. This article is an open access article distributed under the terms and conditions of the Creative Commons Attribution (CC BY) license (https://creativecommons.org/licenses/by/4.0/).

## 1. Introduction

Research on UV photon imaging detectors with high temporal resolution and high spatial resolution would have broad application prospects in many fields [1–4]. In space, where the sky is extremely dark, weak and low-surface-brightness light sources can be observed with ultraviolet detectors. A series of exploration missions have been carried out in space. NASA's International Ultraviolet Explorer conducted very successful spectral studies of light sources with wavelengths of 120–335 nm, followed by far-ultraviolet spectroscopic detection using a high-sensitivity large-size photon-counting array [5,6]. The Institute for Astronomy and Astrophysics in Tubingen is developing and building photon-counting microchannel plate imaging detectors using coplanar XS anodes and advanced low-power readout electronics with a 128-channel charge amplifier chip device [7]. The detectors of the Extreme Universe Space Observatory's multi-wavelength telescope use photomultiplier tubes to study atmospheric phenomena and have single-photon-counting sensitivity [8].

In ultraviolet photon imaging detectors, charge division anodes occupy the position of the core device. Charge division anodes determine the location of events by dividing the MCP charge cloud among multiple electrode channels. Compared with other anodes, the XS anode has the advantages of a higher spatial resolution, higher count rate, good linearity, and low gain requirements [9–15]. However, the traditional methods of making anodes include laser cutting [3] and printing [12]. The general sizes of these two processing

techniques for laser cutting are 20 × 20 mm and 30 × 30 mm, of which it is difficult to achieve a large-area array [9,11]. Moreover, the splicing method is complicated with multiple square anodes. Berkeley Lab uses high-temperature co-fired ceramics to process anodes [16], but the temperature of high-temperature co-fired calcination is above 1500° and the processing method is relatively complicated. At present, the application demand for large-area arrays is relatively high [13,17]. Therefore, we proposed a single-layer XS anode processed using Printed Circuit Board (PCB) technology, which can reduce costs and achieve large-area array detection. Moreover, we study the output of the electron cloud from the MCP to the final signal collected by the anode plate. The quality of the signal will affect the quality of the final resolution.

XS anode imaging detectors often require optimization of the event charge footprint for high spatial resolution and good image linearity [18]. In order to achieve better detector performance indicators, the electron cloud footprint characteristics can be optimized by changing the geometry and specific parameters of the XS anode. At the same time, we need to consider that the single layer anode will bring inevitable crosstalk [19–21]. Crosstalk is caused by inter-strip capacitance, which affects the charge collection of the strips, adding a certain degree of noise to the output signal. Impulse noise in the anode output signal is added to the electronic readout system, indirectly affecting spatial resolution. The accuracy of the pulse value of the anode output signal enables more precise localization of events and also prevents the pulse signal from being masked by noise from the strip. Therefore, it is necessary to conduct theoretical and simulation research on the parameter design of the XS anode and analyze the parameters of the XS anode based on simulation.

This article mainly proposes a single-layer XS anode using PCB technology and analyzes and optimizes its parameters. Section 2 introduces the working principle of the XS anode detector. Through theoretical research, the movement principle of electrons on the metal strips, the equivalent model of the interaction between the charge cloud and the XS anode, and the capacitance between the XS anode strips are given. Section 3 simulates the XS anode, establishes a three-dimensional finite element model, studies the effects of the strip width, strip distance width, and electron vertical diffusion distance of the XS anode on the charges collected by the horizontal and vertical strips, and analyzes the crosstalk between different strips. From the perspective of optimizing the XS anode charge distribution and inter-strip capacitance, anode parameters such as strip width and insulation thickness are designed. In Section 4, with the help of the model described in this paper, the manufacturing process of the anode is improved. At the same time, based on the results of theoretical simulation, a single-layer XS anode based on PCB technology was designed and processed, which can reduce costs and achieve large area array detection. In Section 5, we build a test system. The designed anodes were tested and compared with the simulation results. The small difference between the measured and simulated values proved the accuracy of the model.

## 2. Theory and Simulation of XS Anode

### *2.1. Subsection*

According to the general Shockley–Ramo rule [22], to theoretically analyze and calculate the charge collection efficiency under different electrode structures, as shown in Figure 1, when electrons move around the conductor at a speed $v$, the induced current $I_a$ in the electrode can be calculated by the following formula,

$$I_a = -q\frac{E_a \cdot u}{V_a} \quad (1)$$

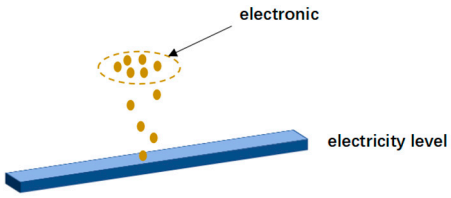



**Figure 1.** Electronic collection model.

In the formula, $E_a$ is the electric field at the position of the charged particle when the applied voltage of the strip is $V_a$. For multiple electrodes, when calculating the induced current of charged particles in a certain electrode, it is necessary to apply a voltage $V_a$ on the electrode and set the voltages of other electrodes to 0; $u$ is the speed of electrons in vacuum. As the particles pass through the electrodes, an equal and opposite charge to the charge on the electron is induced onto the electrode surface.

### *2.2. Anode Theoretical Model*

Using the comsol 6.1 simulation software, we studied the model of the interaction between the charge cloud and the XS anode, and the equivalent diagram of the XS anode model is shown in Figure 2. The solid line represents the capacitance between adjacent strips, and the dashed line represents the coupling capacitance between all strips. When simulating the XS anode, some simplifications and assumptions were made to the model. The first is the number of strips. There are 32 horizontal strips and 32 vertical strips, respectively, since the simulation of 64 strips requires a large amount of computation and complicated grid division, the calculation requirements for creating a sufficiently detailed grid are very high. We simulated using five horizontal electrodes and five vertical electrodes so that the footprint of the electron cloud can be covered and any electric field effect or charge effect during the electron movement can be observed.

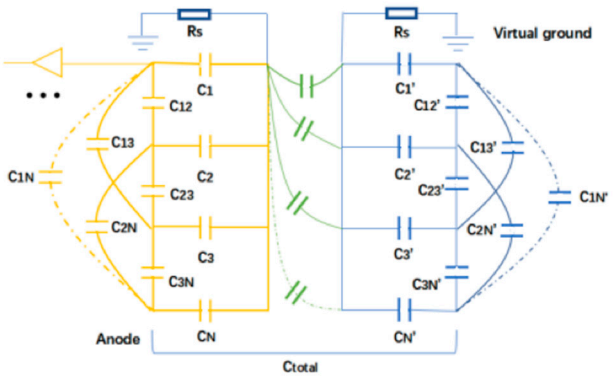


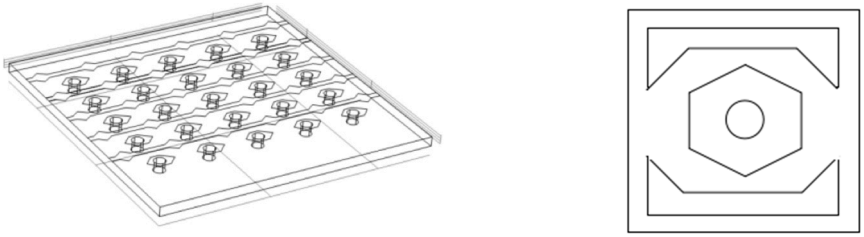

**Figure 2.** Equivalent diagram of XS anode model.

The photons incident on the MCP are converted into photoelectrons by the photocathode. Under the action of high voltage, the photoelectrons are multiplied by the MCP to form an electron cloud. The multiplied electron cloud passes a certain distance and is received by the XS anode. The electron cloud roughly satisfies the Gaussian distribution. The charge density of the electron cloud can be approximated [23] as

$$\sigma(x,y) = \frac{q}{\pi r_i^2} exp(\frac{-(x^2+y^2)}{r_i^2}) \quad (2)$$

A traditional cross-strip anode consists of two layers: one for the X dimension and one for the Y dimension. The geometry designed in this article uses a single layer of strip XS anode with the strip array located on the front side of a thin PCB. The anode is divided into transverse electrodes and longitudinal electrodes, which are used for the position encoding

of two sets of events. The anode converts the received electrons into charges, which are transmitted to 32 horizontal strips and 32 vertical strips, respectively. The model diagram of the XS anode is shown in Figure 3a. And, Figure 3b is the smallest unit of the designed single anode shape, which is composed of horizontal strips and 32 vertical strips. The horizontal electrodes are strip-shaped and the shape of the vertical electrode is a hexagonal pad, and the horizontal and vertical receiving areas are 1:1 to ensure that the signal pickup amplitude on each layer is almost equal. This is designed to improve the ability to resolve "multiple hit" events. For pulsed sources or high-rate operation, it is beneficial to increase the count rate.



(**a**) (**b**)

**Figure 3.** Anode model. (**a**) XS anode equivalent model, (**b**) XS anode minimum unit.

The charge value at each strip is determined by the numerical integration of the charge density over the strip area. The XS anode scheme uses the charge detected on each strip to determine the charge cloud centroid for each strip. The size of the charge cloud should be optimized so that it covers multiple strips to obtain the best spatial resolution. The charges collected on the strips are sensed by charge-sensitive amplifiers connected individually to each strip. The preamplified signal from each strip is then digitized using two 32-channels and interfaced to a PC. Each recorded photon is represented by a set of digitized strip signal amplitudes Qi. Two MCPs which produce a 'chevron' stack were placed a distance d above the XS anode, and a potential of 200 V was applied between the MCP output and the XS anode to provide an accelerating electric field. Through this model, we can more fully understand the specific movement process of electrons on the anode.

### *2.3. Crosstalk Effect of the Inter-Electrode Capacitance*

The main factor that affects the resolution of the detector is electronic noise. Electronic noise is mainly generated by charge-sensitive amplifiers and signal input capacitors. For single-layer XS anodes, there will be capacitive coupling between strips, which interferes with adjacent strip signals and reduces strip signals, thereby reducing the signal-to-noise ratio and thus affecting the resolution of the XS anode.

Total capacitive load on the amplifier input:

$$C_{in} = C_i + C_{ie} + C_a + (1 + A) \cdot C_f + C_p \tag{3}$$

In the formula, $C_i$ is the strip capacitance, $C_{ie}$ is the capacitance between different strips, $C_a$ is the amplifier input capacitance, $C_f$ is the feedback capacitance, $C_p$ is parasitic capacitance, and $A$ is the gain of the open circuit charge sensitive amplifier. Generally speaking, the feedback capacitance is very small (only a few pf), and the capacitance $C_{ie}$ between the strips will affect the collected signal. The greater the crosstalk, the less accurate the signal will be, thus reducing the resolution.

$$N = N_0 + N_c C_{in} \tag{4}$$

$N_0$ is the preamplifier noise without capacitive load, and $N_c$ is the average electronic noise. By calculating the inter-electrode capacitance, the electronic noise-limited spatial resolution of the XS anode detector can be estimated.

$$Q_m = Q - Q_i = Q - 2VC_i \tag{5}$$

$$Q = 2VC_i + C_{dyn}V \tag{6}$$

$$V = \frac{Q}{2C_I + C_{dyn}} \tag{7}$$

$$Q_m = Q - \frac{2QC_i}{2C_I + C_{dyn}} \tag{8}$$

$C_{dyn}$ is considered to be the dynamic capacitance of the charge-sensitive amplifier. From Formula (8), it can be known that when $C_{dyn} >> C_i$, the capacitance of the external electrode to ground can be approximated as $C_i$. The charge $Q_m$ measured by the amplifier is equal to the total charge $Q$ minus the charge $Q_i$ lost to the outside of the strips. It can, thus, be seen that a large dynamic capacitance will ensure minimum charge loss, yielding maximum signal-to-noise ratio, thereby maximizing the efficiency of the electronic device and improving resolution.

For an ideal XS anode, the relationship between capacitance $C$, charge $Q$, and potential $V$ is

$$Q = C_{mutual}V, Q = \begin{bmatrix} Q_1 \\ \vdots \\ Q_n \end{bmatrix}, C_{mutual} = \begin{bmatrix} C_{11} & \cdots & C_{1n} \\ \vdots & \ddots & \vdots \\ C_{n1} & \cdots & C_{nn} \end{bmatrix}, V = \begin{bmatrix} V_1 \\ \vdots \\ V_n \end{bmatrix} \tag{9}$$

However, high efficiency signal transmission is also very important in practical applications. Fundamentally speaking, analyzing and solving the crosstalk problem generated during signal transmission is essentially a problem of solving Maxwell's equations under certain boundaries and excitation conditions. The expression for the charge on the strips can be written as the Maxwell capacitance matrix:

$$Q' = C_{maxavell}V, Q' = \begin{bmatrix} Q'_1 \\ \vdots \\ Q'_n \end{bmatrix}, C_{maxavell} = \begin{bmatrix} \sum_{i=1}^{n} C_{1i} & \cdots & -C_{1n} \\ \vdots & \ddots & \vdots \\ -C_{n1} & \cdots & \sum_{i=1}^{n} C_{ni} \end{bmatrix} \tag{10}$$

In the formula, $C_{ii}$ is the capacitance of i horizontal strips and 32 vertical strips to the vacuum chamber, $C_{ij}$ is the capacitance between band i horizontal strips and j vertical strips, and $C_{ij} = C_{ji}$. Substituting Formula (10) into Formula (9), the relationship between ideal charge and actual charge can be obtained, and the charge can be corrected to eliminate crosstalk.

$$Q' = C_{maxwell}C_{mutual}^{-1}Q \tag{11}$$

## 3. Simulation Results and Discussion

### 3.1. Dynamic Properties of Charge Density

The dynamic characteristics of the surface charge density of the XS anode were studied, as shown in Figure 4. The electron cloud follows a Gaussian distribution on the anode, and the electrons are collected by horizontal strips and vertical strips. The diffusion radius of the electron cloud increases with the distance d. On the one hand, a charge cloud that is too narrow can cause image distortion. On the other hand, excessive diffusion of charge cloud footprints can lead to distortion at the edges of the image, resulting in a reduction in the

signal-to-noise ratio and thus in resolution. The number of strips we want to cover is 3–5, so we want the distance between the MCP and the anode to be as small as possible, but the actual distance also needs to be considered. So, we chose the distance of d to be 0.5–2 mm.

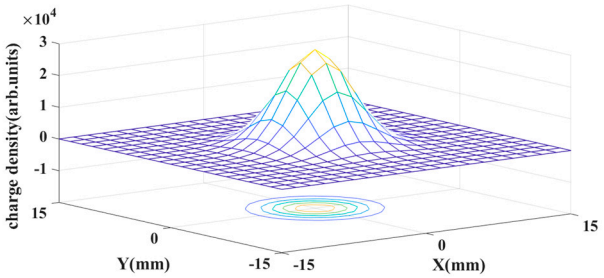



**Figure 4.** The surface charge density of the XS anode.

### *3.2. Optimization of XS Anode Parameters*

The relationship between the collected charge of the horizontal and vertical strips and the receiving area is shown in Figure 5. At different emission distances d, by changing the width and distance of the horizontal strips and the vertical strips, different proportions of receiving areas are obtained. Obviously, the charge ratio decreases with the increase in d, increases with the increase in the receiving area, and the rate increases. It can be seen that the singlelayer XS anode designed in this paper has a high charge collection efficiency. When the receiving area ratio s of the horizontal and vertical strips is 1, d is 2 mm and the charge ratio approaches 1. Furthermore, inaccuracies in charge collection can affect image distortion during imaging. That is, each of the horizontal and vertical electrodes receive half of the charge from mcp. This means more charge from the MCP charge footprint will be collected by the anode and less charge can be lost.

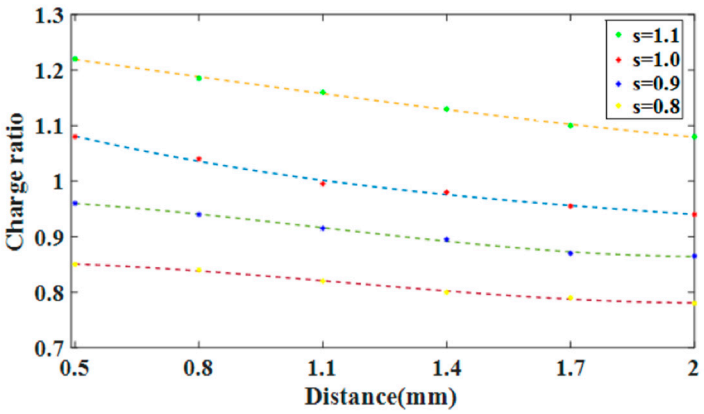



**Figure 5.** The change in charge ratio with distance L under different area ratios. The area ratios of four XS anodes with different sizes are 0.8, 0.9, 1.0, 1.1.

### *3.3. Crosstalk between Strips*

This section shows the simulation of crosstalk between different strips of the XS anode, as shown in Figure 6. The capacitance between the horizontal and vertical strips of XS anodes of different sizes was calculated. It can be seen from the figure that the inter-strip capacitance is between 2 and 8 pF. Under the same substrate thickness, the inter-strip capacitance increases as the strip width increases. In addition, for the same strip width, the capacitance between strips decreases as the substrate thickness increases. Reducing the capacitance between electrodes can reduce crosstalk. Low strip capacitance is achieved by using extremely thick substrates. Under the same conditions with other anode parameters, increasing the anode period can reduce the strip capacitance of the anode. However, the period size of the anode is also limited by the size of the electron cloud reaching the anode.

Therefore, the design requirements and detector structural parameters must be considered comprehensively during actual design. Through simulation, we found that when the substrate thickness is 120 µm, w1 is 110 µm, and w2 is 530 µm, the crosstalk is small.

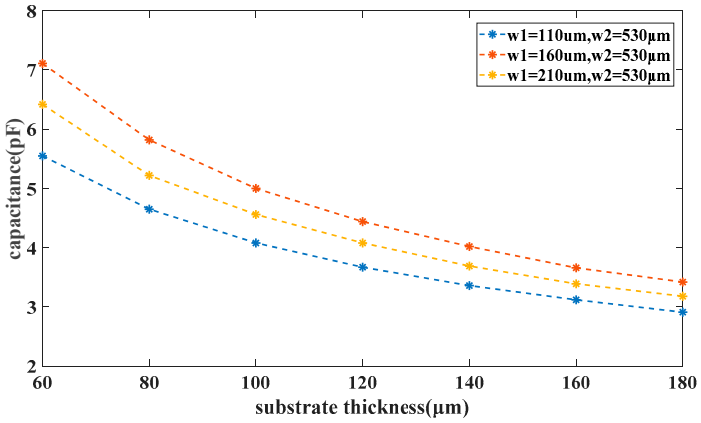



**Figure 6.** Variation of capacitance with substrate thickness.

## 4. Experimental Setup

MCP uses two plates made of lead silicate glass with a bias angle of 10°. The plates are stacked one on top of the other, arranged in a "V" configuration, with the top plate coated with CsI to improve quantum detection efficiency. A bias resistor is connected across the MCP stack to provide gain stability, and a resistor connected from the MCP output to ground provides the electric field for the charge cloud to pass through the MCP output to the anode, as shown in Figure 7.

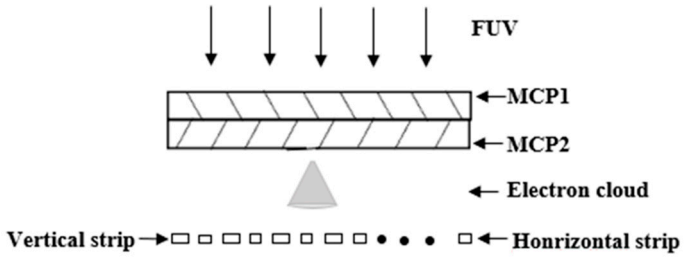



**Figure 7.** Schematic diagram of anode receiving signal.

*Cross-Strip Anode Design*

The XS anode designed in this paper is a single-layer structure; that is, the horizontal strip and the vertical strip are located on the same layer plane. The receiving area of the horizontal strip and the vertical strip is 1:1. The horizontal strip directly collects the charge signal to a section of the strip and then transmits the signal. The vertical strip transmits the charge signal through the via hole. Part of the horizontal strip is a protruding triangle, and the shape of the vertical strip is a hexagon. The purpose of this is to receive electrons more accurately, and the receiving surface of the horizontal and vertical electrodes is 1:1 to improve the electron collection ability. The charge cloud generated by the MCP spans about five periods of the XS anode strip. The resulting charge measured from each strip is used for the centroid of the cloud position with less precision than the width of a single anode, satisfying the required high spatial resolution. At the same time, the PCB manufacturing process is adopted, and the manufacturing is simple and the cost is low.

## 5. Experimental Results and Discussion

### *5.1. Actual Measurement*

Figure 8 shows the actual picture of the XS anode produced. The XS anode bases are all rogers (εr = 2.2). The XS anode is designed and manufactured from the PCB process. The traditional upper and lower strips are processed on the same plane, divided into horizontal strips and vertical strips, which can avoid the upper stripe from blocking the lower strip which can be made into large area array detectors. At the same time, it can also avoid the upper electrode from blocking the lower electrode, improve charge collection efficiency, and improve SNR. The specific parameters of the strip production are shown in Table 1.

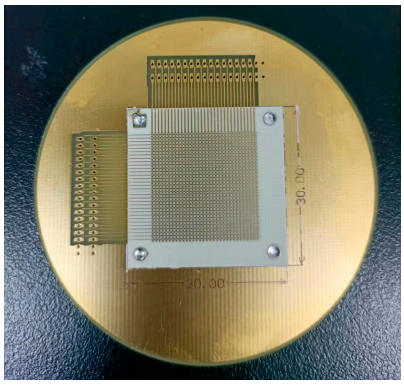


**Figure 8.** XS anode physical picture.

**Table 1.** XS anode electrode production parameters.

| Strip Width | Strip Distance | Periodic Width | Area Ratio | Strip Thickness |
|---|---|---|---|---|
| 110 μm | 530 μm | 640 μm | 1:1 | 120 μm |

### *5.2. XS Anode Test*

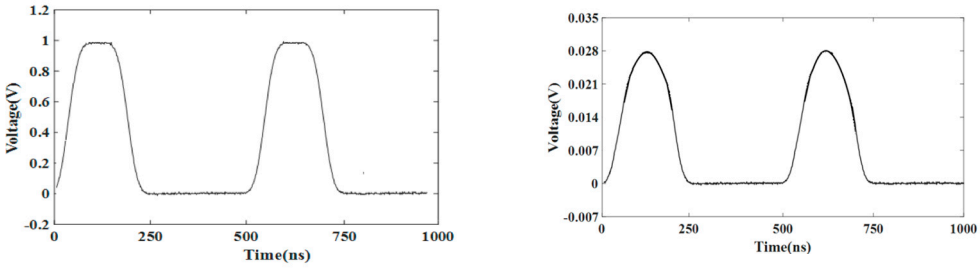
In order to prove the XS anode performance test, a test circuit was built which was divided into five parts: a signal generator, oscilloscope, reference ground plane, XS anode, and terminal. We used a signal generator and oscilloscope to test the anode signal. A charge of 1000 pC was injected above the anode, and then the charge signal at the signal collection end of the horizontal and vertical strips was tested. The test results are shown in Table 2. The approximate ratio of horizontal and vertical strips is 1:1. This may be caused by the space charge distribution. The total charge collected is less than 1000 pC, probably because electrons can be ejected in any direction. Therefore, some signal may be lost as electrons fly upward away from the plate instead of downward into the plate. In terms of anode design, the maximum amount of charge can be collected.

**Table 2.** Charge collected.

| Charge | Horizontal Strip Charge | Vertical Strip Charge |
|---|---|---|
| 1000 pC | 380 pC | 350 pC |

Then, the crosstalk is tested. We study induced pulses at adjacent strips when signals within the event pulse time range are transmitted through one strip. The ground plane is used to eliminate noise signals including space radiation interference, and the high-impedance probe is used to reduce the influence of the test equipment on the parasitic parameters of the device under test. Then, a periodic pulse signal is output through the Tektronix 3011 signal generator. The pulse rise time is 10 ns and the pulse amplitude is 1 V. Finally, the Agilent 5032 A wave detector is used to display the transmission signal on the interfering line and the crosstalk signal on the interfered line and compare the impact

level of crosstalk under different conditions (see Figure 9a). It can be seen from the test results in Figure 9 that the crosstalk on adjacent lines is very obvious; the peak-peak value of the induced signal of the far-end adjacent strip reaches 28 mv. The crosstalk signal has a smaller pulse amplitude than the main signal. Therefore, we conclude that appropriate selection of parameters will reduce crosstalk.




(**a**) (**b**)

**Figure 9.** Crosstalk test results: (**a**) input signal, (**b**) output signal test results from adjacent strips.

## 6. Conclusions

This paper mainly discusses the factors that affect the signal at the anode front end of the detector. A single-layer XS anode structure was designed based on PCB technology and a finite element simulation was performed on the electron cloud behind the anode to study the factors affecting charge collection and the crosstalk caused by parameters between anode strips. It can be seen from the simulation results that this design can collect electrons to the greatest extent. When the electron cloud covers 5 strips, crosstalk can be minimized by reducing the distance d and increasing the thickness of the substrate. Based on the simulation results and actual processing technology, a cross-strip anode with a period length of 650 μm, a strip width of 110 μm, an insulation width of 0.5 mm, and a period number of i = j = 32 was designed and prepared. The test results are consistent with the simulation results, which proves the reliability of the model. This paper provides an effective basis for the realization of low-cost, easy-to-process, and large-area high-resolution ultraviolet single-photon imaging detectors.

**Author Contributions:** Conceptualization, J.D. and Y.Y.; methodology, J.D. and J.Z.; software, J.D.; validation, J.D., Y.Y. and Y.S.; formal analysis, J.D. and A.L.; investigation, J.D. and Y.S.; resources, J.D.; data curation, J.D.; writing—original draft preparation, J.D.; writing—review and editing, J.D., J.Z. and Y.Y.; visualization, J.D.; supervision, J.D., J.Z., Y.Y. and Y.B.; project administration, J.Z., Y.Y. and Y.B.; funding acquisition, J.Z., Y.Y. and Y.B. All authors have read and agreed to the published version of the manuscript.

**Funding:** This work was supported by the National Natural Science Foundation of China, the Scientific Instrument Developing Project of the Chinese Academy of Sciences and the West Light Foundation of the Chinese Academy of Sciences under Grant No. 12027803, Grant No.GJJSTD20220006 and Grant No. XAB2022YN12.

**Institutional Review Board Statement:** Not applicable.

**Informed Consent Statement:** Not applicable.

**Data Availability Statement:** The data presented in this study are available on request from the corresponding author. The data are not publicly available due to organizational privacy.

**Conflicts of Interest:** The authors declare no conflict of interest.

## References

1. Tremsin, A.; Lebedev, G.V.; Siegmund, O.H.W.; Vallerga, J.; McPhate, J.B.; Hussain, Z. High-resolution detection system for time-of-flight electron spectrometry. *Nucl. Instrum. Methods Phys. Res. Sect. A* **2007**, *582*, 172–174. [CrossRef]
2. Siegmund, O.H.W.; Welsh, B.; Vallerga, J.; Tremsin, A.; McPhate, J. High-performance microchannel plate imaging photon counters for spaceborne sensing. *Proc. SPIE* **2006**, *6220*, 622004.

3. Tremsin, A.; Siegmund, O.H.W.; Vallerga, J.; Hull, J.S.; Abiad, R. Cross-strip readouts for photon counting detectors with high spatial and temporal resolution. *IEEE Trans. Nucl. Sci.* **2004**, *51*, 1707–1711. [CrossRef]
4. Zhang, X.; Chen, B. Wide-field auroral imager onboard the Fengyun satellite. *Light Sci. Appl.* **2019**, *45*, 3957–3960. [CrossRef]
5. Martin, D.C.; Fanson, J.; Schiminovich, D.; Morrissey, P.; Friedman, P.G.; Barlow, T.A.; Conrow, T.; Grange, R.; Jelinsky, P.N.; Milliard, B.; et al. The Galaxy Evolution Explorer: A Space Ultraviolet Survey Mission. *Astrophys. J.* **2005**, *619*, L1–L4. [CrossRef]
6. Medallon, S.; Welty, D. *STIS Instrument Handbook*, Version 22.0; STScI: Baltimore, MD, USA, 2023.
7. Conti, L.; Barnstedt, J.; Buntrock, S.; Diebold, S.; Hanke, L.; Kalkuhl, C.; Kappelmann, N.; Kaufmann, T.; Rauch, T.; Stelzer, B.; et al. Microchannel-Plate Detector Development for Ultraviolet Missions. *arXiv* **2020**, arXiv:2012.12548.
8. Casolino, M.; Barghini, D.; Battisti, M.; Blaksley, C.; Belov, A.; Bertaina, M.; Bianciotto, M.; Bisconti, F.; Blin, S.; Bolmgren, K.; et al. Observation of night-time emissions of the earth in the near UV range from the international space station with the mini-EUSO detector. *Remote Sens. Environ.* **2023**, *284*, 113336. [CrossRef]
9. Murakami, G.; Yoshioka, K.; Yoshikawa, I. High-resolution imaging detector using five microchannel plates and a resistive anode encoder. *Appl. Opt.* **2010**, *49*, 2985–2993. [CrossRef]
10. Jagutzki, O.; Lapington, J.S.; Worth, L.; Spillman, U.; Mergel, V.; Schmidt-Böcking, H. Position sensitive anodes for MCP read-out using induced charge measurement. *Nucl. Instrum. Methods Phys. Res. Sect. A* **2004**, *477*, 256–261. [CrossRef]
11. Siegmund, O.H.W.; Vallerga, J.; Jelinsky, P.; Redfern, M.; Michalet, X.; Weiss, S. Cross delay line detectors for high time resolution astronomical polarimetry and biological fluorescence imaging. *IEEE. Nucl. Sci.* **2005**, *1*, 448–452.
12. Diebold, S.; Barnstedt, J.; Hermanutz, S.; Kalkuhl, C.; Kappelmann, N.; Pfeifer, M.; Schanz, T.; Werner, K. UV MCP Detectors for WSO-UV: Cross Strip Anode and Readout Electronics. *IEEE Trans. Nucl. Sci.* **2013**, *60*, 918–922. [CrossRef]
13. Vallerga, J.; McPhate, J.; Tremsin, A.; Siegmund, O.H.W.; Raffanti, R.; Cumming, H.; Seljak, A.; Virta, V.; Varner, G. Development of a flight qualified 100 × 100 mm MCP UV detector using advanced cross strip anodes and associated ASIC electronics. *Proc. SPIE* **2016**, *9905*, 99053F.
14. Vallerga, J.; Raffanti, R.; Cooney, M.; Cumming, H.; Varner, G.; Seljak, A. Cross strip anode readouts for large format, photon counting microchannel plate detectors: Developing flight qualified prototypes of the detector and electronics. *Proc. SPIE* **2014**, *9144*, 91443J.
15. Vallerga, J.; Raffanti, R.; Tremsin, A.; Siegmund, O.H.W.; McPhate, J.; Varner, G. Large-format high-spatial resolution cross-strip readout MCP detectors for UV astronomy. *Proc. SPIE* **2010**, *7732*, 773203.
16. Siegmund, O.H.W.; Curtis, T.L.; McPhate, J.B.; Vallerga, J. High performance cross strip imaging readout Planacon sealed tubes. *Nucl. Instrum. Methods Phys. Res. Sect. A* **2023**, *1049*, 168077. [CrossRef]
17. Bezrukov, L.B.; Grabmayr, P.; Greiner, D.; Jochum, J.; Lubsandorzhiev, B.; Lubsandorzhiev, N.; Poleshuk, V. Large area photodetectors for astroparticle physics Cherenkov arrays: PMTs vs. HPDs. *Nucl. Instrum. Methods Phys. Res. Sect. A* **2011**, *639*, 65–69. [CrossRef]
18. Lei, F. Research on the Key Technology of Single Photon Imaging Based on Position Sensitive Anode. Ph.D. Dissertation, Xi'an Institute of Optics and Precision Mechanics, University of Chinese Academy Sciences, Xi'an, China, 2019.
19. Xing, Y.; Chen, B.; Zhang, H.J.; Wang, H.-F.; He, L.-P.; Jin, F.-Y. Calculating and optimizing inter-electrode capacitances of charge division microchannel plate detectors. *Nucl. Instrum. Methods Phys. Res. Sect. A* **2016**, *814*, 82–89. [CrossRef]
20. Angelico, E.; Seiss, T.; Adams, B. Capacitively coupled pickup in MCP-based photodetectors using a conductive metallic anode. *Nucl. Instrum. Methods Phys. Res. Sect. A* **2017**, *846*, 75–80. [CrossRef]
21. Riegler, W.; Burgarth, D. Signal propagation, termination, crosstalk and losses in resistive plate chambers. *Nucl. Instrum. Methods Phys. Res. Sect. A* **2002**, *481*, 130–143. [CrossRef]
22. Ramo, S. Currents induced electron motion. *Proc. IRE* **1939**, *27*, 584–585. [CrossRef]
23. Dias, T.H.V.T.; Santos, F.P.; Conde, C.A.N. The primary electron cloud in xenon for X-rays in the 0.1 to 10 keV range. *Nucl. Instrum. Methods Phys. Res. Sect. A* **1991**, *310*, 137–139. [CrossRef]


**Disclaimer/Publisher's Note:** The statements, opinions and data contained in all publications are solely those of the individual author(s) and contributor(s) and not of MDPI and/or the editor(s). MDPI and/or the editor(s) disclaim responsibility for any injury to people or property resulting from any ideas, methods, instructions or products referred to in the content.